PAPER

# Photon echo using imperfect x-ray pulse with phase fluctuation

IOP Publishing Physica Scripta
Phys. Scr. 94 (2019) 105508 (8pp) https://doi.org/10.1088/1402-4896/ab1785

# Photon echo using imperfect x-ray pulse with phase fluctuation

**Jin-Fu Chen**[1,2], **Hui Dong**[2] and **Chang-Pu Sun**[1,2]

[1] Beijing Computational Science Research Center, Beijing 100193, People's Republic of China
[2] Graduate School of China Academy of Engineering Physics, No. 10 Xibeiwang East Road, Haidian District, Beijing, 100193, People's Republic of China

E-mail: hdong@gscaep.ac.cn

Received 20 December 2018, revised 1 April 2019
Accepted for publication 9 April 2019
Published 8 August 2019

**Abstract**

We study the impact of inter-pulse phase fluctuation in an x-ray free-electron laser on the signal in photon echo spectroscopy, which is one of the simplest nonlinear spectroscopic methods. A two-pulse echo model is considered with two-level atoms as the sample. The effect of both fluctuation amplitude and correlation strength of the random phase is studied both numerically and analytically. We find that the random phase leads to the changed amplitude and the unchanged rephasing time of the photon echo signal, and show that the relaxation time can be obtained with a previous photon echo setup by an additional average across the signals in different repeated measurements for the pulses with random phase.

Keywords: photon echo, phase fluctuation, x-ray free-electron laser

(Some figures may appear in colour only in the online journal)

## 1. Introduction

The recent development of x-ray source, especially the large facility x-ray free-electron laser (XFEL), has attracted widespread attention [1–3] toward detecting properties beyond the scope of traditional instruments. The unique features of the high brightness, short pulse duration, and frequency range of the XFEL light source open a new era in the scientific investigation of atomic, molecular physics, and biology [3–5]. One potential application is the implementation of nonlinear spectroscopy [6–11] to investigate the dynamics of matter in extreme conditions. Nonlinear spectroscopy typically requires a high degree of temporal coherence [12, 13], i.e. inter-pulse phase stability as well as intra-pulse stability [13]. However, pulses generated from many current facilities, may not fulfill such requirement due to its inter-pulse phase fluctuation [3, 14, 15, 17, 16, 18, 19]. A direct question is how such phase fluctuation affects the actual signal, especially on methods of extracting key parameters, e.g. the relaxation time. Photon echo and time-delayed four-wave mixing have been studied in previous works theoretically and experimentally [20–25], which showed that the signal for the strong pulses is quite different from that of the weak pulses.

We will investigate the impact of inter-pulse phase fluctuation of x-ray pulses on photon echo based on the Wei–Norman algebraic method [26, 27]. Photon echo is one of the simplest nonlinear spectroscopy methods, yet fundamental to many advanced spectroscopic methods, e.g. two-dimensional electronic spectroscopy and two-dimensional vibrational spectroscopy [12, 13]. Photon echo [28–30] is an optical analogy to spin echo, and is designed to remove ensemble average for measuring properties of individual spins while maintaining signal amplitude by avoiding measuring individuals directly [12]. Taking a simple two-level system as an example, an excitation pulse creates an initial state $|\psi(0)\rangle = \alpha|g\rangle + \beta|e\rangle$, where $|g\rangle$ and $|e\rangle$ are the ground and excited state with energies 0 and $\epsilon_e$, respectively. The free evolution brings the system to the state $|\psi(t)\rangle = \alpha|g\rangle + \beta\exp(-i\epsilon_e t)|e\rangle$. A subsequent $\pi$ pulse reverses the population $|\psi'(t)\rangle = \alpha|e\rangle + \beta\exp(-i\epsilon_e t)|g\rangle$. The later evolution compensates the phase accumulated during the evolution of the ensemble between the two pulses, namely, $|\psi(T, t)\rangle = \alpha\exp(-i\epsilon_e T)|e\rangle + \beta\exp(-i\epsilon_e t)|g\rangle$. At a revival time $T = t$, the impact of disorder (inhomogeneity) over the signal is essentially removed. However, it is usually not easy to achieve the $\pi$ pulse due to the weak pulse intensity in the

 

optical region. One solution is to use non-collinear incident pulses in order to separate the echo signal from other signals via the phase matching method, which is frequently adopted in nonlinear spectroscopy studies [12].

In this paper, we show the general model of measuring the signal of two-pulse photon echo on the ensemble of two-level atoms with an imperfect x-ray pulse. Based on the Wei–Norman algebraic method [26, 27], it is feasible to calculate the photon echo signal for strong pulses with the random phase effect. The amplitude $\mathcal{A}$ of the photon echo signal is obtained analytically for weak random phase effect. Finally, we provide the method used to measure the relaxation time of the system for the pulses with random phase.

## 2. Photon echo with an imperfect x-ray pulse

In the current paper, we consider an ensemble of two-level atoms with the ground state $|g\rangle$ and the excited state $|e\rangle$. The free Hamiltonian for the two-level atom is

$$H_0 = \epsilon_e|e\rangle\langle e|, \tag{1}$$

where we have set the energy of the ground state as $\epsilon_g = 0$. The energy levels here are inner-shell electronic states [9], accessible with the frequency of XFEL. The interaction Hamiltonian between pulses and the atom is given by the dipole interaction $H_I = -\vec{\mu}\cdot\vec{E}(t)$, where $\vec{\mu}$ is the transition dipole and $\vec{E}(t)$ is the electric field of the incident x-ray pulse. Under the rotating wave approximation, the interaction Hamiltonian for a pulse with central frequency $\nu_0$ and wave vector $\vec{k}$ is simplified as

$$H_I = -\Omega(t)e^{-i\nu_0 t - i\phi(t) + i\vec{k}\cdot\vec{r}}|e\rangle\langle g| + h.c., \tag{2}$$

where $\phi(t)$ characterizes the random phase of the x-ray pulse, $\vec{r}$ is the spatial location of the atom, and $\Omega(t)$ is the Rabi frequency. We simplify the model with the square pulse approximation: the strength of the pulse is a constant $\Omega$ in the duration for the pulse and diminishes when the pulse ends.

Here, we consider the two-pulse photon echo, and the two pulses are set to be resonated to the atom $\nu_0 = \epsilon_e$. The model and the two-pulse-echo are shown in figure 1. The first pulse interacts with the atoms with the duration $\delta\tau_1$, while the second pulse interacts with the atoms with the duration time $\delta\tau_2$ after delay time $\tau$ of the end of the first pulse. The evolution matrices for each pulse are $U_i(\vec{k}_i, \delta\tau_i)(i = 1, 2)$, and the free evolution of the atom is $U_0(t_f, t_i) = U_0(t_f - t_i) = \exp[-iH_0(t_f - t_i)]$, where $t_i(t_f)$ is the initial (final) time of the free evolution. The final wave function of the atom at delay time $T$ is obtained as

$$|\psi(T, \tau)\rangle = U_0(T)U_2(\vec{k}_2, \delta\tau_2)U_0(\tau)U_1(\vec{k}_1, \delta\tau_1)|\psi_0\rangle, \tag{3}$$

where the initial state $|\psi_0\rangle$ is usually considered as the ground state $|\psi_0\rangle = |g\rangle$. To derive the evolution matrices $U_i(k_i, \delta\tau_i)$ for each pulse, we rewrite the Hamiltonian in the interacting picture as

$$\hat{H}_I(t) = -\begin{pmatrix} 0 & \hbar\Omega e^{i\phi(t) - i\vec{k}\cdot\vec{r}} \\ \hbar\Omega e^{-i\phi(t) + i\vec{k}\cdot\vec{r}} & 0 \end{pmatrix}. \tag{4}$$

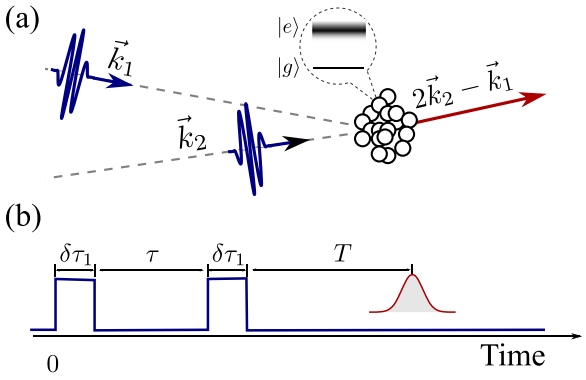


**Figure 1.** The model and the pulse sequence. (a) The two incident pulses are directed to the sample in a non-collinear geometry along two directions $\vec{k}_1$ and $\vec{k}_2$. The emission of the two-pulse photon echo is along the direction $2\vec{k}_2 - \vec{k}_1$. The sample is an ensemble of two-level atoms with the ground state $|g\rangle$ and excited state $|e\rangle$. The blurred line of the excited state shows the fluctuation of the energy $\epsilon_e$ between the ground state and the excited state. (b) The blue line shows the two pulses, and the red line shows the signal. The duration of the two pulses are $\delta\tau_1$ and $\delta\tau_2$, and the delay time is $\tau$. Also, the measurement of the echo signal acts at $T$ time after the end of the second pulse.

The time dependence of equation (4) only comes from the random phase factor $\phi(t)$. With the following definitions:

$$H_1(\vec{k}) = \begin{pmatrix} 0 & \hbar\Omega e^{-i\vec{k}\cdot\vec{r}} \\ \hbar\Omega e^{i\vec{k}\cdot\vec{r}} & 0 \end{pmatrix}, \tag{5}$$

$$H_2(\vec{k}) = \begin{pmatrix} 0 & -i\hbar\Omega e^{-i\vec{k}\cdot\vec{r}} \\ i\hbar\Omega e^{i\vec{k}\cdot\vec{r}} & 0 \end{pmatrix}, \tag{6}$$

$$H_3(\vec{k}) = \begin{pmatrix} \hbar\Omega & 0 \\ 0 & -\hbar\Omega \end{pmatrix}, \tag{7}$$

$\hat{H}_I(t)$ is rewritten in a compact form

$$\hat{H}_I(t) = -\cos[\phi(t)]H_1 + \sin[\phi(t)]H_2. \tag{8}$$

The three operators $H_l$ $(l = 1, 2, 3)$ satisfy the commutation relation of angular momentum operators $[H_i(\vec{k}), H_j(\vec{k})] = 2i\hbar\sum_{l=1}^{3}\Omega H_l(\vec{k})\epsilon_{ijl}$. Following the Wei–Norman algebraic method [26, 27], the evolution matrix for a pulse is written as

$$\hat{U}_{\vec{k},\phi}(t, 0) = e^{-i\chi_3(t)H_3}e^{-i\chi_2(t)H_2}e^{-i\chi_1(t)H_1}, \tag{9}$$

where $\vec{k}$ is the wave vector and $\phi$ is a certain realization of the random phase. With the commutation relation of $H_l$ $(l = 1, 2, 3)$, we have derived the differential equations for the time-dependent parameters $\{\chi_l(t)\}$, $(l = 1, 2, 3)$ in appendix A

$$\begin{cases} \dot{\chi}_3 = -\cos(\phi + 2\chi_3\Omega)\tan 2\chi_2\Omega \\ \dot{\chi}_2 = \sin(\phi + 2\chi_3\Omega) \\ \dot{\chi}_1 = -\cos(\phi + 2\chi_3\Omega)\sec 2\chi_2\Omega. \end{cases} \tag{10}$$

The initial condition is $\chi_l(0) = 0$, $l = 1, 2, 3$. The nonlinear time-dependent differential equations (10) are accessible to be solved numerically with a given $\phi(t)$.

Next, we change the evolution matrices derived by equation (9) from the interacting picture to the Schrödinger

picture, which is linked by a free evolution $U_1(\vec{k}_1, \delta\tau_1) = U_0(\delta\tau_1)\hat{U}_{\vec{k}_1,\phi_1}(\delta\tau_1, 0)$ and $U_2(\vec{k}_2, \delta\tau_2) = U_0(\delta\tau_2)\hat{U}_{\vec{k}_2,\phi_2}(\delta\tau_2, 0)$. $U_0(\delta\tau_i)$ is absorbed to the free evolution part or neglected when $\delta\tau_i$ is small compared to the interval time $\tau$ and the measurement time $T$. According to equation (9), the evolution matrix $\hat{U}_{\vec{k}_1,\phi_1}(\delta\tau_1, 0)$ and $\hat{U}_{\vec{k}_2,\phi_2}(\delta\tau_2, 0)$ for the first pulse and second pulse is written with $\chi_l$ and $\zeta_l$, $l = 1, 2, 3$, respectively. Combined with equation (3), the echo term is derived by sorting terms with the phase factor matching $\exp[i(2\vec{k}_2 - \vec{k}_1)\cdot\vec{r}]$ as follows:

$$\begin{aligned}\langle\psi(T,\tau)|\ \mu_t|\psi(T,\tau)\rangle \sim\ & i\mu^* e^{-i(T-\tau)\epsilon_e} e^{i(2\vec{k}_2-\vec{k}_1)\cdot\vec{r}} \\ & \times \frac{e^{2i\Omega(\zeta_3-\chi_3)}}{8}[\sin((\zeta_2+\zeta_1)\Omega) + i\sin((\zeta_2-\zeta_1)\Omega)]^2 \\ & \times [\sin(2(\chi_2-\chi_1)\Omega) + 2i\sin(2\chi_1\Omega) \\ & + \sin(2(\chi_2+\chi_1)\Omega)].\end{aligned} \tag{11}$$

For the ensemble of atoms, their energy $\epsilon_e$ between the ground state and the excited state has fluctuations for the inhomogeneous broadening, assumed as Gaussian distribution with mean value $\epsilon_0$ and variance $\sigma_0^2$ with the following form:

$$p(\epsilon_e) = \frac{1}{\sqrt{2\pi}\,\sigma_0}\exp\left[-\frac{(\epsilon_e-\epsilon_0)^2}{2\sigma_0^2}\right]. \tag{12}$$

We consider that the duration time $\delta\tau_i$ of the two pulses is much shorter than the inverse of the standard deviation $1/\sigma_0$. In this situation, the atoms resonate to the pulses mainly contribute to the final signal of the photon echo, and the summation over transition energies of different molecules contributes a Gaussian decay with $(T - \tau)$, namely,

$$\sum_{\epsilon_e} e^{-i(T-\tau)\epsilon_e} \to e^{-\frac{1}{2}\sigma_0^2(T-\tau)^2 - i(T-\tau)\epsilon_0}. \tag{13}$$

At the revival time $T = \tau$, the average over different molecules vanishes so that the relaxation time can be directly detected. The amplitude $\mathcal{A}$ of the photon echo signal is the square of the absolute value of equation (11)

$$\begin{aligned}\mathcal{A} = & \frac{|\mu|^2 e^{-\sigma_0^2(T-\tau)^2}}{64}[\sin^2((\zeta_2+\zeta_1)\Omega) + \sin^2(\zeta_2-\zeta_1)\Omega]^2 \\ & [(\sin(2(\chi_2-\chi_1)\Omega) + \sin(2(\chi_2+\chi_1)\Omega))^2 \\ & + 4\sin^2(2\chi_1\Omega)].\end{aligned} \tag{14}$$

For the ideal case with no random phase ($\phi(t) =$ constant), we obtain the amplitude

$$\mathcal{A}_{\text{ideal}} = \frac{|\mu|^2 e^{-\sigma_0^2(T-\tau)^2}}{4}\sin^4(\Omega\delta\tau_2)\sin^2(2\Omega\delta\tau_1) \tag{15}$$

with $\chi_2^{(0)} = \chi_3^{(0)} = \zeta_2^{(0)} = \zeta_3^{(0)} = 0$, $\chi_1^{(0)} = -\delta\tau_1$, $\zeta_1^{(0)} = -\delta\tau_2$. It is clear that the random phase only affects the amplitude of the photon echo. A factor $\mathcal{F}$ is defined to represent the value of the amplitude

$$\begin{aligned}\mathcal{F} = & \{\sin^2[(\zeta_2+\zeta_1)\Omega] + \sin^2[(\zeta_2-\zeta_1)\Omega]\}^2 \\ & \times[[\sin[2(\chi_2-\chi_1)\Omega] + \sin[2(\chi_2+\chi_1)\Omega]]^2 \\ & + 4\sin(2\chi_1\Omega)^2].\end{aligned} \tag{16}$$

In the following discussion, we consider that the two pulses are the same except with different directions, namely, $\delta\tau_1 = \delta\tau_2 = \delta\tau$, and $\chi_i = \zeta_i$ $(i = 1, 2, 3)$. For the case without phase fluctuation ($\phi(t) =$ constant), the factor $\mathcal{F}$ is simply

$$\mathcal{F}_{\text{ideal}} = 16\sin^4(\Omega\delta\tau)\sin^2(2\Omega\delta\tau). \tag{17}$$

In figure 2(a), we show the distribution of the signal intensity $\mathcal{A}$ as a function of $T$. The random phase elicits fluctuation to the signal and affects the average value. In the simulation, we generate the random function $\phi(t)$ with the Ornstein–Uhlenbeck process. The average of $\phi(t)$ is zero $\langle\phi(t)\rangle = 0$, and its two-point correlation function satisfies

$$\langle\phi(t_1)\phi(t_2)\rangle = \Phi^2 e^{-\gamma|t_1-t_2|}, \tag{18}$$

where $\Phi$ is the fluctuation amplitude of the random phase and $\gamma$ is the correlation strength. The amplitude of the signal is evaluated via equation (11) with $\chi_i$ and $\zeta_i$, which is numerically solved with the differential equation (10). In the simulation, we have chosen parameter set as $\tau = 20$, $\sigma_0^2 = 0.1$, $\Omega = 1$, $\delta\tau = 0.8$, $\gamma = 0.2$, and $\Phi = 2$. The statistics are calculated with 10 000 repeats of the current process by generating different random functions $\phi(t)$ for each parameter set. In figure 2(a), we show the average signal with a green dashed line, the most probable signal with an orange dashed line, and the ideal signal without random phase with a red dotted line. We further show the randomness of the factor $\mathcal{F}$ figure 2(b), whose distribution $p(\mathcal{F})$ is not Gaussian. It is clear that the random phase induces fluctuation on the strength of the signal of the photon echo.

With the observation of the randomness of the echo amplitude, it is meaningful to calculate the average signal with different repeats. Here, we try to derive perturbation results for the average amplitude $\langle\mathcal{A}\rangle$ with random phase. We consider that the random phase is small and apply the approximation $\cos\phi(t) \approx 1$, $\sin\phi(t) \approx \phi(t)$ to obtain the linear differential equation of equation (10) for $\chi_2$ and $\chi_3$ as follows. The differential equation for $\chi_1$ is kept for second order to obtain the signal amplitude to the second order

$$\begin{cases}\dot{\chi}_3 = -2\Omega\chi_2 \\ \dot{\chi}_2 = \phi + 2\Omega\chi_3 \\ \dot{\chi}_1 = -1 + \frac{1}{2}(\phi + 2\chi_3\Omega)^2 - \frac{1}{2}(2\chi_2\Omega)^2.\end{cases} \tag{19}$$

Now, the current equation (19) has an integral solution

$$\begin{aligned}\chi_3(t) &= -\int_0^t \sin 2\Omega(t-t_1)\phi(t_1)\mathrm{d}t_1 \\ \chi_2(t) &= \int_0^t \cos 2\Omega(t-t_1)\phi(t_1)\mathrm{d}t_1 \\ \chi_1(t) &= -t + \int_0^t \frac{1}{2}\phi^2 + 2\Omega\chi_3\phi + 2\Omega^2\chi_3^2 - 2\Omega^2\chi_2^2\mathrm{d}t_1.\end{aligned} \tag{20}$$

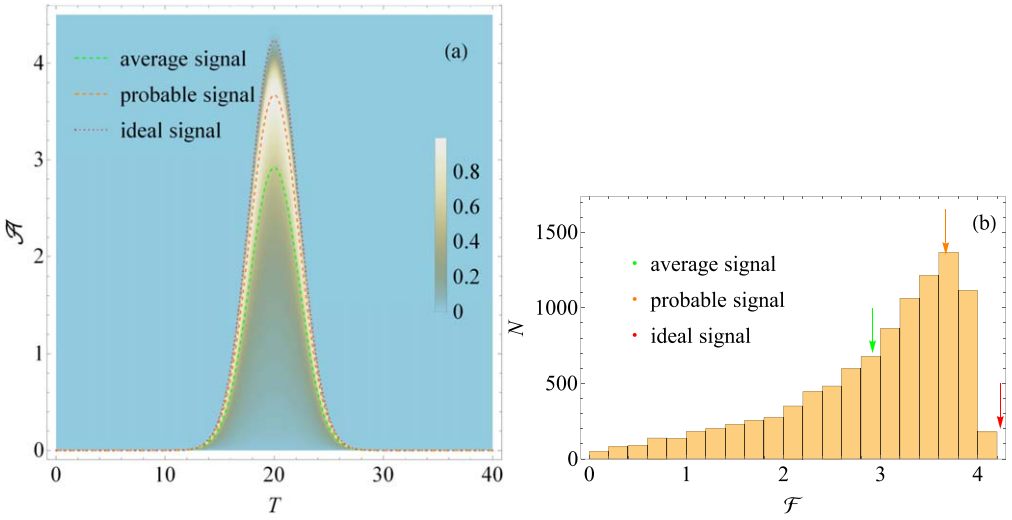


**Figure 2.** The photon echo signal and the distribution of strength factor $\mathcal{F}$. The parameters are chosen as $\tau = 20$, $\sigma_0^2 = 0.1$, $\Omega = 1$, $\delta\tau = 0.8$, $\gamma = 0.2$, and $\Phi = 2$. (a) The distribution of the signal at time $T$. The color shows the probability at given time $T$ with the amplitude $\mathcal{A}$. The green curve and the orange curve shows the average signal and the most probable signal, respectively, while the red curve shows the ideal echo signal without any phase randomness. (b) The distribution of the strength factor $\mathcal{F}$ with 10 000 repeats for the echo signal at $T = \tau$. The arrows show the average, most probable, and ideal signal with the same color scheme as in figure 2(a).

For small random phase $\phi(t)$, we expand the factors $\chi_i$, $i = 1$, 2, 3 to their first order $\chi_i = \chi_i^{(0)} + \chi_i^{(1)}$, where $\chi_i^{(0)}$ is the average value, i.e., $\chi_1^{(0)} = 0$, $\chi_2^{(0)} = 0$, $\chi_3^{(0)} = -\delta\tau$ and $\chi_i^{(1)}$ gives the fluctuation due to the random phase. We obtain the explicit form of the factor $\mathcal{F}$ under the perturbation formalism

$$\mathcal{F} = \mathcal{F}_{\text{ideal}} - 128\chi_1^{(1)}\Omega\sin^5(\delta\tau\Omega)(2\cos(\delta\tau\Omega) + \cos(3\delta\tau\Omega)) + 64(\chi_2^{(1)})^2\Omega^2\sin^4(\delta\tau\Omega)\cos(2\delta\tau\Omega)(2\cos(2\delta\tau\Omega) + 1). \tag{21}$$

Equation (21) contains $\chi_2^{(1)}$ to the second order and $\chi_1^{(1)}$ to the first order. It is verified numerically that $\chi_1^{(1)}$ is as the same order as $(\chi_2^{(1)})^2$ in appendix B, and they are both the lowest order contributing to $\mathcal{F}$.

The factor $\mathcal{F}$ is a random variable due to the random phase $\phi(t)$. We derive the average value $\langle(\chi_2^{(1)})^2\rangle$ and $\langle\chi_1^{(1)}\rangle$ by the two-point correlation function. The detailed calculation is presented in appendix B. The analytical result for the mean value of $\mathcal{F}$ becomes

$$\langle\mathcal{F}\rangle = \mathcal{F}_{\text{ideal}} + 64\Omega^2\sin^4(\delta\tau\Omega)\cos(2\delta\tau\Omega)(2\cos(2\delta\tau\Omega) + 1)\langle(\chi_2^{(1)})^2\rangle - 128\Omega\sin^5(\delta\tau\Omega)(2\cos(\delta\tau\Omega) + \cos(3\delta\tau\Omega))\langle\chi_1^{(1)}\rangle. \tag{22}$$

In figures 3(a) and 4(a), we plot the average signal $\langle\mathcal{F}\rangle - \mathcal{F}_{\text{ideal}}$ as a function of the fluctuation amplitude $\Phi$ with the correlation strength $\gamma$ fixed. In these figures, red dots show the exact result by numerical calculation, and the lines represent the analytical result in equation (22). For small fluctuation amplitude $\Phi$, the analytical result matches the numerical calculation well, as illustrated in the subsets of figures 3(a) and 4(a). However, the analytical result deviates from exact numerical result for large $\Phi$, e.g. $\Phi > 0.2$ as shown in figure 3(a) or $\Phi > 1.5$ as shown in figure 4(a). In figures 3(b) and 4(b), we plot the average signal $\langle\mathcal{F}\rangle - \mathcal{F}_{\text{ideal}}$ as a function of the correlation strength $\gamma$ with the fluctuation amplitude $\Phi$ fixed. The analytical result matches the numerical calculation well whether for large or small $\gamma$.

In the above discussion, we have shown the random phase effect on the signal amplitude of an ensemble of two-level atoms without any decoherence. The key function of photon echo is to measure the relaxation time $\tau_r$. In open systems, the environment induces a decoherence to the atoms, which contributes to the decreasing of the non-diagonal term $\rho_{eg}(t) = \exp[-i\epsilon_e t - t/\tau_r]$. With the decoherence effect, the signal derived in equation (16) becomes

$$\mathcal{A}_{\text{open}} = \frac{|\mu|^2 e^{-\sigma_0^2(T-\tau)^2-(T+\tau)/\tau_r}}{64}\mathcal{F}. \tag{23}$$

At the revival time $T = \tau$, the average signal is

$$\langle\mathcal{A}_{\text{open}}\rangle = |\mu|^2\exp(-2\tau/\tau_r)\langle\mathcal{F}\rangle. \tag{24}$$

With fixed $\delta\tau$ and the given random phase, the average for the factor $\mathcal{F}$ is invariant. To measure the relaxation time $\tau_r$, we still follow the previous photon echo setup of changing the delay time $\tau$ and obtain the signal amplitude at $T = \tau$. By taking the average over different repeats, the relaxation time is recovered via equation (24).

Currently, the experimental setup of x-ray photon echo is achievable with the split-delay approach [31, 32], where the x-ray pulse is split by a silicon beam splitter [32]. The change to the setup in [31] is to direct the split two pulses to the sample along two directions. With the split-delay approach, the phase difference between pulses is fixed with delay time. The phase fluctuation of each pulses is theoretically considered in the current paper.

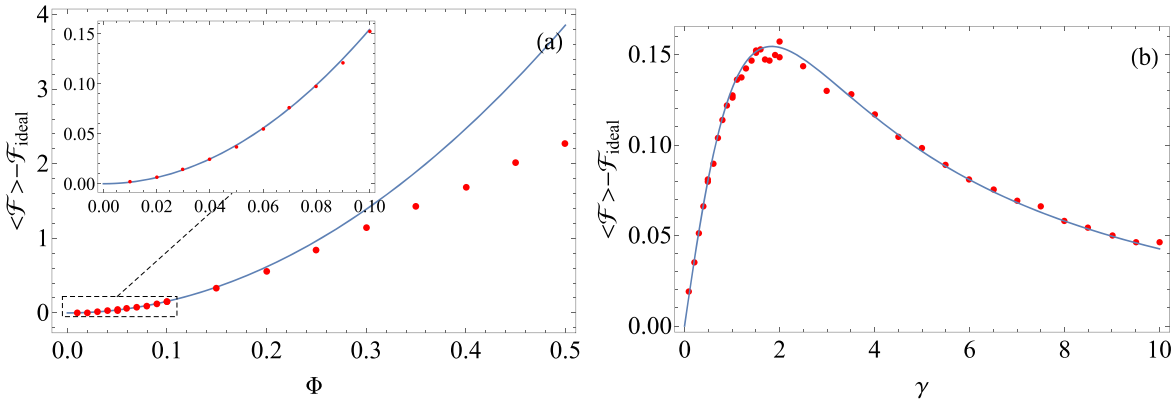


**Figure 3.** The relation between $\langle\mathcal{F}\rangle - \mathcal{F}_{\text{ideal}}$ and the fluctuation amplitude $\Phi$ and the correlation strength $\gamma$. The parameters are chosen as $\Omega = 1$, $\delta\tau = 4.75$, and $\gamma = 1/4.587$ as shown in figure 3(a) and $\Phi = 0.05$ as shown in figure 3(b). The red points show the numerical calculation and the solid curve shows the analytical result.

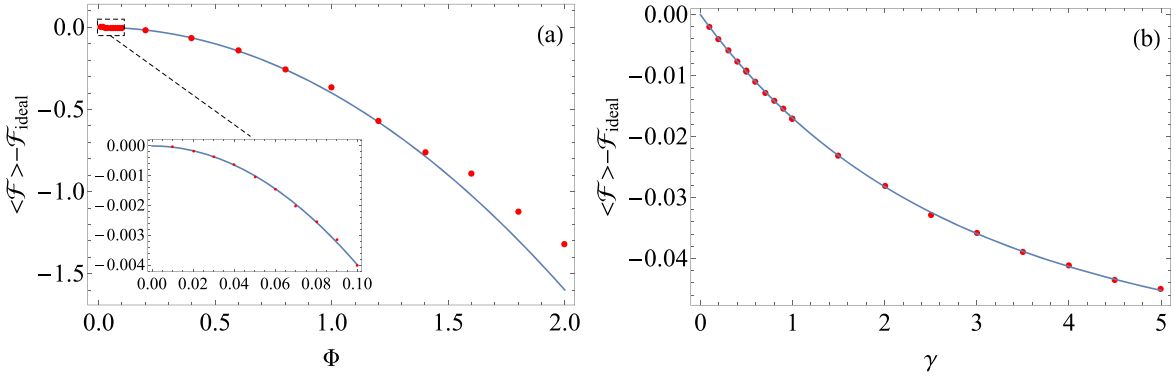


**Figure 4.** The relation between $\langle\mathcal{F}\rangle - \mathcal{F}_{\text{ideal}}$ and the fluctuation amplitude $\Phi$ and the correlation strength $\gamma$. The parameters are chosen as $\Omega = 1$, $\delta\tau = 0.8$, and $\gamma = 0.2$ as shown in figure 4(a) and $\Phi = 0.1$ as shown in figure 4(b). The red points show the numerical calculation and the solid curve shows the analytical result.

## 3. Conclusion

We have theoretically calculated the impact of phase randomness on the photon echo experiment, which is fundamental to many other nonlinear spectroscopy, such as two-dimensional spectroscopy. In the current paper, we find that the phase randomness will induce fluctuation in the photon echo signal, yet not affect the rephasing time. By averaging the signal from different repeats, the relaxation time can be measured by changing the delay time between the first and the second pulse. Our results suggest that the x-ray photon echo might be realized on XFEL. Our non-perturbative approach for the photon echo will be utilized later for the design of a photon echo experiment and the analyses of the observed photon echo signal.

## Acknowledgments

This work is supported by NSFC (Grants Nos. 11421063 and 11534002), the National Basic Research Program of China (Grant Nos. 2016YFA0301201 and 2014CB921403), and the NSAF (Grant Nos. U1730449 and U1530401).

## Appendix A. Wei–Norman method

In this appendix, we show the detailed derivation of the differential equation (10). The derivation is based on the Wei–Norman algebraic method [26, 27]. The differential of equation (9) is calculated as

$$\begin{aligned}\frac{\mathrm{d}}{\mathrm{d}t}U_{p,\phi}(t,0) = &-i\dot{\chi}_3 H_3 U_{p,\phi}(t,0)\\ &- i\dot{\chi}_2 e^{-i\chi_3 H_3} H_2 e^{-i\chi_2 H_2} e^{-i\chi_1 H_1}\\ &- i\dot{\chi}_1 U_{p,\phi}(t,0) H_1\end{aligned} \tag{A1}$$

with the commutations

$$e^{-i\chi_3 H_3} H_2 e^{i\chi_3 H_3} = H_2 \cos 2\Omega\chi_3 - H_1 \sin 2\Omega\chi_3, \tag{A2}$$

$$\begin{aligned}&e^{-i\chi_3 H_3} e^{-i\chi_2 H_2} H_1 e^{i\chi_2 H_2} e^{i\chi_3 H_3}\\ &= -H_3 \sin 2\Omega\chi_2\\ &+ H_2 \sin 2\Omega\chi_3 \cos 2\Omega\chi_2\\ &+ H_1 \cos 2\hbar\Omega\chi_3 \cos 2\Omega\chi_2.\end{aligned} \tag{A3}$$

Equation (A1) is rewritten as

$$i\frac{\partial}{\partial t}U_{p,\phi}(t,0) = [(\dot{\chi}_3 - \dot{\chi}_1\sin 2\Omega\chi_2)H_3 + (\dot{\chi}_1\sin 2\Omega\chi_3\cos 2\Omega\chi_2 + \dot{\chi}_2\cos 2\Omega\chi_3)H_2 + (\dot{\chi}_1\cos 2\Omega\chi_3\cos 2\Omega\chi_2 - \dot{\chi}_2\sin 2\Omega\chi_3)H_1]U_{p,\phi}(t,0). \tag{A4}$$

The coefficients must match the Schrödinger equation (8)

$$\begin{pmatrix} 0 & -\sin 2\Omega\chi_3 & \cos 2\Omega\chi_3\cos 2\Omega\chi_2 \\ 0 & \cos 2\Omega\chi_3 & \sin 2\Omega\chi_3\cos 2\Omega\chi_2 \\ 1 & 0 & -\sin 2\Omega\chi_2 \end{pmatrix}\begin{pmatrix}\dot{\chi}_3\\ \dot{\chi}_2\\ \dot{\chi}_1\end{pmatrix} = \begin{pmatrix}-\cos\phi\\ \sin\phi\\ 0\end{pmatrix}. \tag{A5}$$

The differential equations are obtained by taking the inverse matrix

$$\begin{cases} \dot{\chi}_3 &= -\cos\phi\cos 2\chi_3\Omega\tan 2\chi_2\Omega \\ & \quad + \sin\phi\sin 2\chi_3\Omega\tan 2\chi_2\Omega \\ \dot{\chi}_2 &= \cos 2\chi_3\Omega\sin\phi + \cos\phi\sin 2\chi_3\Omega \\ \dot{\chi}_1 &= -\cos\phi\cos 2\chi_3\Omega\sec 2\chi_2\Omega \\ & \quad + \sin\phi\sec 2\chi_2\Omega\sin 2\chi_3\Omega \end{cases} \tag{A6}$$

With further simplification, we obtain equation (10).

## Appendix B. The calculation of $\langle(\chi_2^{(1)})^2\rangle$ and $\langle\chi_1^{(1)}\rangle$

Here, we give the detailed calculation for $\langle(\chi_2^{(1)})^2\rangle$ and $\langle\chi_1^{(1)}\rangle$. With equation (20), we can calculate the average value of $(\chi_2^{(1)})^2$

$$\langle(\chi_2^{(1)})^2\rangle = \int_0^{\delta\tau}\int_0^{\delta\tau}\cos 2\Omega(t-t_1)\cos 2\Omega(t-t_2) \times \langle\phi(t_1)\phi(t_2)\rangle\,\mathrm{d}t_2\,\mathrm{d}t_1. \tag{B1}$$

The result of the integral gives

$$\langle(\chi_2^{(1)})^2\rangle = \Phi^2\left(\frac{\gamma\delta\tau}{\gamma^2+4\Omega^2} + \frac{2\gamma e^{-\gamma\delta\tau}(\gamma\cos(2\delta\tau\Omega) - 2\Omega\sin(2\delta\tau\Omega))}{(\gamma^2+4\Omega^2)^2} + \frac{\gamma\sin(4\delta\tau\Omega) - 2\Omega\cos(4\delta\tau\Omega)}{4\Omega(\gamma^2+4\Omega^2)} + \frac{8\Omega^2-6\gamma^2}{4(\gamma^2+4\Omega^2)^2}\right). \tag{B2}$$

The calculation of the average value of $\chi_1^{(1)}$is similar, i.e.

$$\langle\chi_1^{(1)}\rangle = \left\langle\int_0^{\delta\tau}\left(\frac{1}{2}\phi^2 + 2\Omega\chi_3\phi + 2\Omega^2\chi_3^2 - 2\Omega^2\chi_2^2\right)dt_1\right\rangle. \tag{B3}$$

The result is

$$\langle\chi_1^{(1)}\rangle = \Phi^2\left(\frac{\gamma^2\delta\tau}{2\gamma^2+8\Omega^2} - \frac{2\gamma\Omega e^{-\gamma\delta\tau}(\gamma\sin(2\delta\tau\Omega) + 2\Omega\cos(2\delta\tau\Omega))}{(\gamma^2+4\Omega^2)^2} + \frac{\Omega\sin(4\delta\tau\Omega) - \gamma\sin^2(2\delta\tau\Omega)}{2(\gamma^2+4\Omega^2)} + \frac{4\gamma\Omega^2}{(\gamma^2+4\Omega^2)^2}\right). \tag{B4}$$

We also show that the numerical calculation matches the analytical result in figures B1 and B2, which shows that $\langle(\chi_2^{(1)})^2\rangle$ and $\langle\chi_1^{(1)}\rangle$ are the same order and should be kept for the perturbation.

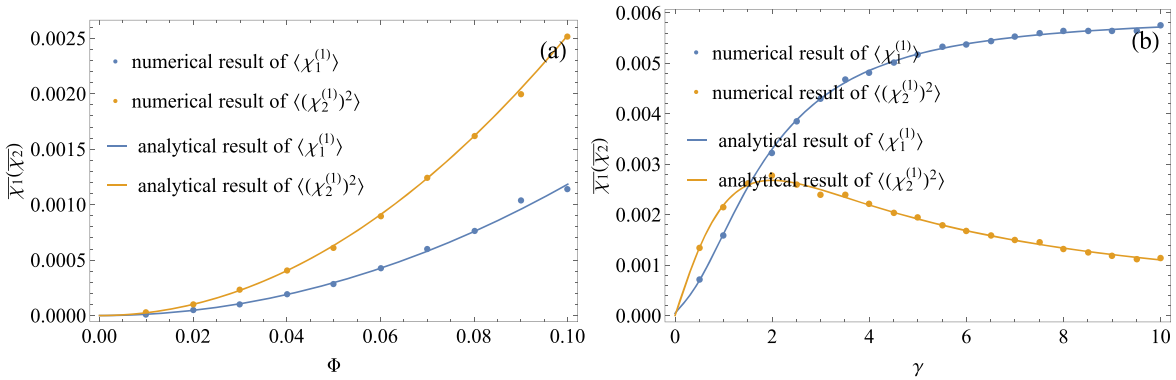


**Figure B1.** The numerical and analytical result of $\langle\chi_1^{(1)}\rangle$ and $\langle(\chi_2^{(1)})^2\rangle$. The parameters are chosen as $\Omega = 1$, $\delta\tau = 4.75$, and $\gamma = 1/4.587$ as shown in figure B1(a) and $\Phi = 0.05$ as shown in figure B1(b). The dot shows the numerical calculation of the average value, and the line shows the analytical result.

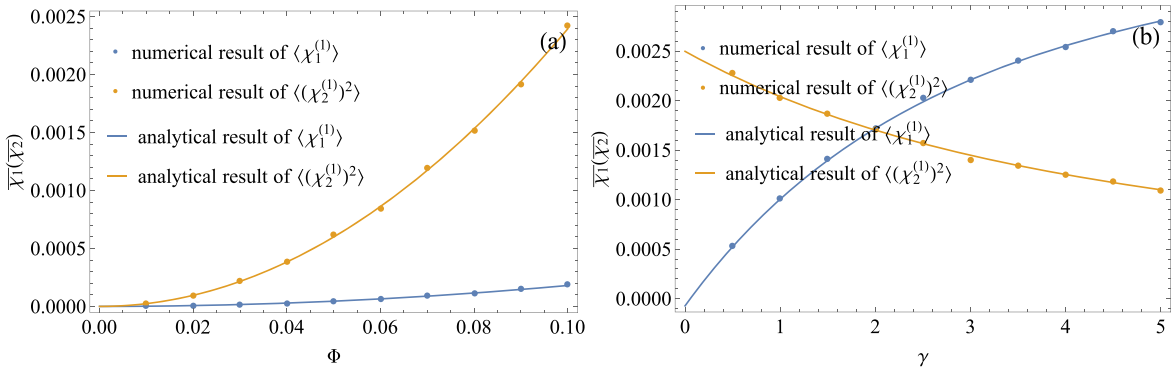


**Figure B2.** The numerical and analytical results of $\langle\chi_1^{(1)}\rangle$ and $\langle(\chi_2^{(1)})^2\rangle$. The parameters are chosen as $\Omega = 1$, $\delta\tau = 0.8$, and $\gamma = 0.2$ as shown in figure B2(a), and $\Phi = 0.1$ as shown in figure B2(b). The dot shows the numerical calculation of the average value, and the line shows the analytical result.

## ORCID iDs

Jin-Fu Chen https://orcid.org/0000-0002-7207-969X

## References


[1] Ullrich J, Rudenko A and Moshammer R 2012 Free-electron lasers: new avenues in molecular physics and photochemistry *Annu. Rev. Phys. Chem.* **63** 635–60

[2] Serkez S, Geloni G, Tomin S, Feng G, Gryzlova E V, Grum-Grzhimailo A N and Meyer M 2017 Overview of options for generating high-brightness attosecond x-ray pulses at free-electron lasers and applications at the European XFEL *J. Opt.* **20** 024005

[3] Bostedt C, Boutet S, Fritz D M, Huang Z, Lee H J, Lemke H T, Robert A, Schlotter W F, Turner J J and Williams G J 2016 Linac coherent light source: the first five years *Rev. Mod. Phys.* **88** 015007

[4] Lindau I 1997 Condensed matter physics using a coherent x-ray source *Nucl. Instrum. Methods Phys. Res., Sect.* A **398** 65–8

[5] Prat E, Löhl F and Reiche S 2015 Efficient generation of short and high-power x-ray free-electron-laser pulses based on superradiance with a transversely tilted beam *Phys. Rev. ST Accel. Beams* **18** 100701

[6] Mukamel S 2005 Multiple core-hole coherence in x-ray four-wave-mixing spectroscopies *Phys. Rev.* B **72** 235110

[7] Schweigert I V and Mukamel S 2007 Coherent ultrafast core-hole correlation spectroscopy: x-ray analogues of multidimensional NMR *Phys. Rev. Lett.* **99** 163001

[8] Schweigert I V and Mukamel S 2008 Double-quantum-coherence attosecond x-ray spectroscopy of spatially separated, spectrally overlapping core-electron transitions *Phys. Rev.* A **78** 052509

[9] Mukamel S, Healion D, Zhang Y and Biggs J D 2013 Multidimensional attosecond resonant x-ray spectroscopy of molecules: lessons from the optical regime *Annu. Rev. Phys. Chem.* **64** 101–27

[10] Healion D, Zhang Y, Biggs J D, Hua W and Mukamel S 2013 Two-dimensional x-ray correlation spectroscopy of remote core states *Struct. Dyn.* **1** 014101

[11] Bennett K, Zhang Y, Kowalewski M, Hua W and Mukamel S 2016 Multidimensional resonant nonlinear spectroscopy with coherent broadband x-ray pulses *Phys. Scr.* **T169** 014002

[12] Mukamel S 1995 *Principles of Nonlinear Optical Spectroscopy* (*Oxford Series in Optical and Imaging Sciences*) vol 6 1st edn (Oxford: Oxford University Press)

[13] Schlau-Cohen G S, Ishizaki A and Fleming G R 2011 Two-dimensional electronic spectroscopy and photosynthesis: fundamentals and applications to photosynthetic light-harvesting *Chem. Phys.* **386** 1–22

[14] Yu L H 1991 Generation of intense UV radiation by subharmonically seeded single-pass free-electron lasers *Phys. Rev.* A **44** 5178–93

[15] Wang J M and Yu L H 1986 A transient analysis of a bunched beam free electron laser *Nucl. Instrum. Methods Phys. Res. Sect.* A **250** 484–9

[16] Lee S, Roseker W, Gutt C, Huang Z, Ding Y, Grübel G and Robert A 2012 High wavevector temporal speckle correlations at the linac coherent light source *Opt. Express* **20** 9790

[17] Yu L-H *et al* 2000 High-gain harmonic-generation free-electron laser *Science* **289** 932–4

[18] Elman U and Kröll S 1996 Statistical modeling and theoretical analysis of the influence of laser phase fluctuations on photon echo data erasure and stimulated photon echoes *Laser Phys.* **6** 721–8

[19] Elman U, Luo B and Kröll S 1996 Influence of laser phase and frequency fluctuations on photon-echo data erasure *J. Opt. Soc. Am.* B **13** 1905

[20] Tchénio P, Débarre A, Keller J-C and Gouët J L L 1989 Optical coherent transients induced by time-delayed correlated broad-bandwidth pulses in the strong-field regime *Phys. Rev.* A **39** 1970–88

[21] Tchénio P, Débarre A, Keller J C and Gouët J L L 1989 Non-Markovian strong-field excitation of optical coherent transients *Phys. Rev. Lett* **62** 415–8

[22] Beach R, DeBeer D and Hartmann S R 1985 Time-delayed four-wave mixing using intense incoherent light *Phys. Rev.* A **32** 3467–74

[23] Finkelstein V and Berman P R 1990 Optical transient signal induced by strong fluctuating pulses *Phys. Rev.* A **42** 3145–8

[24] Finkelstein V 1991 Atomic response to optical fluctuating fields: temporal resolution on a scale less than pulse correlation time *Phys. Rev.* A **43** 4901–12

[25] Friedberg R and Hartmann S R 1988 A diagrammatic technique for calculating radiation of coherently or incoherently excited two-level atoms *J. Phys. B: At., Mol. Opt. Phys.* **21** 683–712

[26] Wei J and E Norman 1963 L algebraic solution of linear differential equations *J. Math. Phys.* **4** 575–81

[27] Sun C P and Xiao Q 1991 Wei–Norman algebraic method solving the evolution of the coherent states of electron in two dimensions* *Commun. Theor. Phys.* **16** 359
[28] Abella I D, Kurnit N A and Hartmann S R 1966 Photon echoes *Phys. Rev.* **141** 391–406
[29] Shvyd'ko Y 2016 X-ray echo spectroscopy *Phys. Rev. Lett.* **116** 080801
[30] Scully M, Stephen M J and Burnham D C 1968 Photon echo in gaseous media *Phys. Rev.* **171** 213–4
[31] Gutt C, Stadler L M, Duri A, Autenrieth T, Leupold O, Chushkin Y and Grübel G 2008 Measuring temporal speckle correlations at ultrafast x-ray sources *Opt. Express* **17** 55
[32] Roseker W, Franz H, Schulte-Schrepping H, Ehnes A, Leupold O, Zontone F, Lee S, Robert A and Grübel G 2011 Development of a hard x-ray delay line for x-ray photon correlation spectroscopy and jitter-free pump-probe experiments at x-ray free-electron laser sources *J. Synchrotron Rad.* **18** 481–91